APC Heartbeats UFIR Smoothing and P-wave Features Analysis using Rice Distribution

CARLOS LASTRE-DOMINGUEZ, YURIY S. SHMALIY, OSCAR IBARRA-MANZANO
Universidad de Guanajuato
Dept. of Electronics Engineering
Carretera Valle de Santiago
Km 3.5 + 1.8, 36885 Salamanca
MEXICO
cm.lastredominguez@ugto.mx; shmaliy@ugto.mx; ibarrao@ugto.mx

Abstract: Heart diseases are one of most frequent causes of death in the modern world. Therefore, the ECG signal features have been under peer review for decades to improve medical diagnostics. In this paper, we provide smoothing of the atrial premature complex (APC) of the electrocardiogram (ECG) signal using unbiased finite impulse response (UFIR) smoothing filtering. We investigate the P-wave distribution using the Rice law and determine the probabilistic confidence interval based on a database associated with normal heartbeats. It is shown that the abnormality in the APC is related to the P-wave morphology. Different filtering techniques employing predictive and smoothing filtering are applied to APC data and compared experimentally. It is demonstrated that UFIR smoothing provides better performance among others. We finally show that the P-wave confidence interval defined for the Rice distribution can be used to provide an automatic diagnosis with a given probability.

Key–Words: Atrial premature complex, UFIR smoothing, electrocardiogram, Rice distribution, confidence interval.

1 Introduction

Electrocardiogram (ECG) signals have been under profound investigation in medical sector for decades and many heart diseases were identified based on ECG. In past decades, methods of statistical signal processing (SSP) were involved to provide accurate decisions. Estimates provided by SSP algorithms strongly depend on confidence intervals (CIs) specified for ECG features [1]. However, measured ECG features are highly variable, because the ECG signals vary depending of the human state and environmental conditions. That imposes difficulties in the recognition heart diseases, among which the arrhythmia is associated with abnormality of the cardiac rhythm [2]. Different types of arrhythmias can be studies analyzing ECG features using SSP. But, in view of measurement noise, optimal algorithms are often required.

The first segment of the ECG signal called 'depolarization' corresponds to the P wave (atrial depolarization). From this feature, the atrial premature complex (APC) can be analysed via changes in the P wave morphology. However, the ECG signal features extraction is a complex process in view of noise and some measurement uncertainties [3–8]. Methods developed in the time and frequency domains include linear predictors, Fourier and wavelet transform-based analysis, etc. [9, 10]. Diverse techniques were also developed to provide noise reduction [11]. In general, denoising algorithms are designed such that the fundamental properties of the ECG signal are not violated. In this regard, optimal smoothing is most powerful due to the best denoising effect and optimal tracking ability. The most widely used smoother was developed by Savitsky and Golay [12]. It provides smoothing at the middle of the averaging horizon. A more general solution is known is the $p-$shift unbiased finite impulse response (UFIR) filter developed by Shmaliy *et al*. [13–15]. This approach implies that lag $q = -p > 0$ must be selected for each degree individually and not obligatorily at the middle of the horizon to provide best denoising. Smoothing filtering is organized here with $p < 0$, filtering with $p = 0$, and predictive filtering with $p > 0$. An optimal Savitsky-Golay smoother minimizing the minimum mean square error (MSE) is given in [16, 17].

In this paper, we apply the p-shift UFIR smoothing filter to ECG data and investigate the confidence interval for the P-wave using the Rice distribution. This investigation is based on the MIT-BIH Arrhythmia Database available for free use from [18, 19].

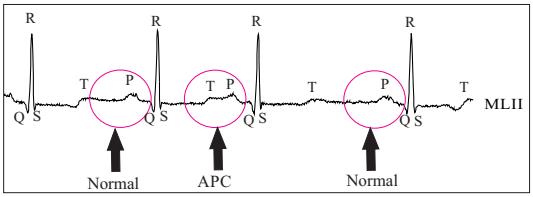

Fig. 1: Typical 'normal' and 'APC' heartbeats from ECG.

1.1 Atrial Premature Complex (APC)

The APC is considered by medical community as a independent predictor of atrial fibrillation, stroke, and death. The frequency of occurrence of APC in the general population is little-known. This abnormality is also related to some other cardiovascular risk factors. The APC is characterized by premature beating originated in the atria and can occur in different situations such as infection, myocardial ishemia, inflamation, usage of tobaco, alcohol, and caffeine, or anxiety and hypokalemia [2]. A fragment of the ECG heartbeats is shown in Fig. (1), in which one recognizes features such as P, QRS complex, and T. As can be seen, the APC is characterized by abnormal P-wave morphology providing a compensatory pause.

2 q-Lag UFIR Smoothing Filtering of Discrete Polynomial ECG Model

Let us define the ECG signal in discrete time index n as x_n and its measurement s_n as

$$s_n = x_n + v_n \,, \tag{1}$$

where v_n is an additive zero mean noise. Because noise is poorly known in such signals. we will ignore its statistics. Signal x_n can be represented with a degree polynomial on a horizon of N points, from $n-N+1-p$ to $n-p$, where $p \lesseqgtr 0$ is a shift such that $p=0$ means filtering, $p<0$ smoothing filtering with lag $q=-p$, and $p>0$ predictive filtering with step p. The p-shift UFIR filter can be designed in the convolution-based batch forms as [20]

$$\hat{x}_{n|n-p} = \sum_{i=1}^{N-1+p} h_{li}(p) s_{n-i} \tag{2}$$

where $h_{ln}(p) \triangleq h_{ln}(N,p)$ is the (N,p)-variant l-degree impulse response of the UFIR filter. In a compact matrix form, (2) can be represented as

$$\hat{x}_{n|n-p} = \mathbf{W}_l^T(p)\mathbf{S}_N \,, \tag{3}$$

where $\mathbf{S}_N$ is the measurement vector and the UFIR filter gain matrix is given by

$$\mathbf{W}_l^T(p) = [\, h_l(p)\, h_{l(1+p)}(p) \cdots h_{l(N-1+p)}(p)\,] \,. \tag{4}$$

In order for the estimate (2) to be unbiased, the following unbiasedness condition must be satisfied,

$$E\{\hat{x}_{n|n-p}\} = E\{x_n\} \,, \tag{5}$$

and the coefficients for gain (4) obeying (5) can be found as shown below.

2.1 p-Shift Gain for UFIR Smoothing Filter

The gain matrix $\bar{\mathbf{W}}_l(p)$ for the UFIR filter has the following fundamental properties:

$$\sum_{i=p}^{N-1+p} h_{li}(N,p) = 1 \,, \tag{6}$$

$$\sum_{i=p}^{N-1+p} h_{li}(N,p) i^u = 0, \quad 1 \le u \le l \,. \tag{7}$$

representing the unit area (6) and zero moments (7). In matrix forms, these properties can be represented by the unbiasedness constraint

$$\bar{\mathbf{W}}_l^T(p)\mathbf{V}(p) = \mathbf{J}^T \,, \tag{8}$$

where

$$\mathbf{J} = [\,1\;0 \cdots 0\,]^T \tag{9}$$

and $\mathbf{V}(p)$ is the $(l+1)\times(l+1)$ Vandermonde matrix,

$$\mathbf{V}(p) = \begin{bmatrix} 1 & p & p^2 \\ 1 & 1+p & (1+p)^2 \\ 1 & 2+p & (2+p)^2 \\ \vdots & \vdots & \vdots \\ 1 & N-1+p & (N-1+p)^2 \end{bmatrix} . \tag{10}$$

By operating the right-side of (8) with an identity $[\mathbf{V}^T(p)\mathbf{V}(p)]^{-1}\mathbf{V}^T(p)\mathbf{V}(p)$ and discarding the nonzero $\mathbf{V}(p)$ from both sides, the p-shift UFIR filter gain becomes

$$\bar{\mathbf{W}}_l^T(p) = \mathbf{J}^T[\mathbf{V}^T(p)\mathbf{V}(p)]^{-1}\mathbf{V}^T(p) \,. \tag{11}$$

The UFIR filter gain can be represented with the l-degree polynomial as [14, 20]

$$h_{ln}(p) = \sum_{j=0}^{l} a_{jl}(p) n^j \,, \tag{12}$$

where coefficient a_{jl} can be defined by solving an equation

$$\mathbf{J} = \mathbf{D}(p)\mathbf{B}(p)\,, \tag{13}$$

where

$$\mathbf{B} = [\,a_{0l}\,a_{1l}\cdots a_{ll}\,]^T \tag{14}$$

and the $(l+1)\times(l+1)$ matrix is

$$\mathbf{D}(p) = \mathbf{V}^T(p)\mathbf{V}(p) = \begin{bmatrix} d_0 & d_1 & \cdots & d_l \\ d_1 & d_2 & \cdots & d_{l+1} \\ \vdots & \vdots & \ddots & \vdots \\ d_l & d_{l+1} & \cdots & d_{2l} \end{bmatrix}, \tag{15}$$

where $d_m(p) = \sum_{i=p}^{N-1} i^m$, $m \in [0, 2l]$, is a generic component. Most frequently, filters of low-degree $l = [1, 4]$ are used with the p-shift polynomial gain existing as [11]

$$h_{li}(N,p) = \begin{cases} \text{nontrivial}, & p \le i \le N-1+p \\ 0, & \text{otherwise} \end{cases}. \tag{16}$$

2.2 Low-Degree Polynomial gains

For linear modeling of ECG signal on $[p, N-1+p]$, the ramp function $h_{1n}(p)$ is used [14],

$$h_{1n}(p) = a_{01}(p) + a_{11}(p)n\,, \tag{17}$$

with the coefficients

$$a_{01}(p) = \frac{2(2N-1)(N-1)+12p(N-1+p)}{N(N^2-1)}\,, \tag{18}$$

$$a_{11}(p) = \frac{6(N-1+2p)}{N(N^2-1)}\,. \tag{19}$$

This gain provides the best noise reduction inherent to simple averaging with lag $q = -p = \frac{N-1}{2}$.

For quadratic and cubic signal models, the polynomial gains are given by

$$h_{2i}(p) = a_{02}(p) + a_{12}(p)i + a_{22}(p)i^2\,, \tag{20}$$

$$h_{3i}(p) = a_{03}(p) + a_{13}(p)i + a_{23}(p)i^2 + a_{33}(p)i^3\,, \tag{21}$$

with the coefficients given in [14, 20].

2.3 Optimized Adaptive Denoising of ECG Signals

An optimal horizon N_{opt} is required by UFIR filtering to minimize the MSE. Because the ECG model is not available, we determine N_{opt} via the measurement residual $s_n - \hat{x}_{n|n-p}(N)$ and the mean square value (MSV)

$$V(N) = E\{[s_n - \hat{x}_{n|n-p}(N)]^2\} \tag{22}$$

by the relation [23]

$$\hat{N}_{\text{opt}} = \arg\min_N \frac{\partial V(N)}{\partial N} + 1\,. \tag{23}$$

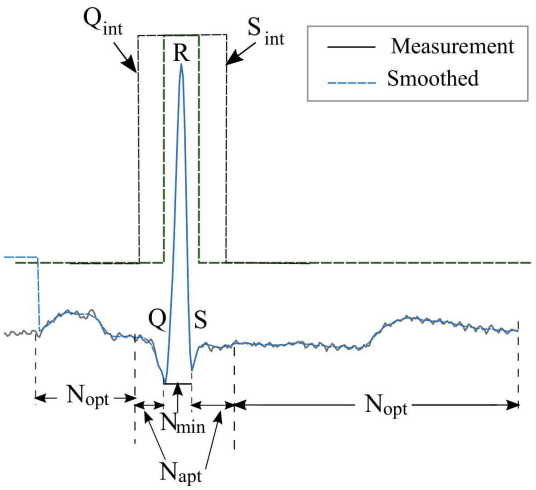

Fig. 2: The ECG signal noisy measurement (sold) and smoothed model (dashed). Optimal N_{opt} is required for slow parts and minimum $N_{\min}$ for the QRS complex. In the algorithm, N varies adaptively between N_{opt} and $N_{\min}$.

The optimal horizon N_{opt} serves for slow parts of the ECG beat shown in Fig. (2), by excluding fast excursions associated with the QSR complex. The MSV V_n behaves similarly for different degrees l and N_{opt} has closely related values for $l = 1, 2, 3$. Because low degrees provide better denoising [23], we select $l = 2$ associated with $N_{\text{opt}} = 21$ (Table 1).

Table 1: Effect of the UFIR degree l on N_{opt} and MSE

	$l=1$	$l=2$	$l=3$	$l=4$
N_{opt}	19	21	20	27
MSE$\times 10^{-4}$	1.7	**1.29**	**1.14**	**0.78**

3 Comparison of Smoothing and Others Techniques

The linear prediction method proposed in [24] and developed for ECG signals by Martis [9] was regarded

as one of the standard approaches to analyse features of digitized ECG signals. A heartbeat x_n is modeled here as a linear combination of its past input samples x_{n-k}, $k = 1, 2, ...p$, where p is considered as the order of prediction and a_k denotes the kth linear prediction coefficient. In the prediction technique, the estimation error is defined as $e_n = x_n - \bar{x}_n$, where the predictive estimate given by $\bar{x}_n$ is computed as $\bar{x}(n) = \sum_{k=1}^{p} a_k x_{n-k}$. According to Martis, e_n is a portion of the ECG signal, which cannot be predicted by linear models. To provide UFIR predictive filtering, we configure the filter degree with $p = 2$ as stated in [25]. The UFIR filter predicts estimates with $p > 0$ and both the prediction method and the UFIR predictive filtering employ the discrete linear prediction of undergoing process via its noisy measurement. Even so, there are some zones in the ECG picture where the linear prediction is not successful in extracting the ECG features. Therefore, a comparative analysis of different methods is required.

In Fig. 3(a), we sketch typical errors produced by the predictive filtering, filtering, and smoothing filtering. A part of the ECG signal taken from [120:200] is zoomed in Fig. 3(b). As can be seen, all filters are successful in denoising the P-wave. However, the UFIR smoothing filter does it more precisely, while the predictive filter is less accurate. The average denoising errors represented with the variance σ^2 are listed in Table 2. This table suggests that the UFIR smoothing filter outperforms both the UFIR filter and the standard linear predictor developed for ECG signals [9].

Table 2: Errors produced by the UFIR smoothing filter, linear predictor, and UFIR predictive filter

Estimator	Average Error	σ^2
Smooth-UFIR	$\mathbf{1.7997 \times 10^{-5}}$	$\mathbf{4.2073 \times 10^{-5}}$
Linear predictor	-0.0074	$2.1462 \times 10^{-}4$
predict UFIR	$-2.4691 \times 10^{-}4$	$2.2799 \times 10^{-}4$

4 P wave Detection

The known technique for ECG signal features extraction is based on the Pan Tompkings algorithm [26]. In this section, we develop another one based on the UFIR smoothing filtering algorithm.

The QRS complex (Fig.2) is the first to detect. To this end, the peak value R (ECG signal maximum) is

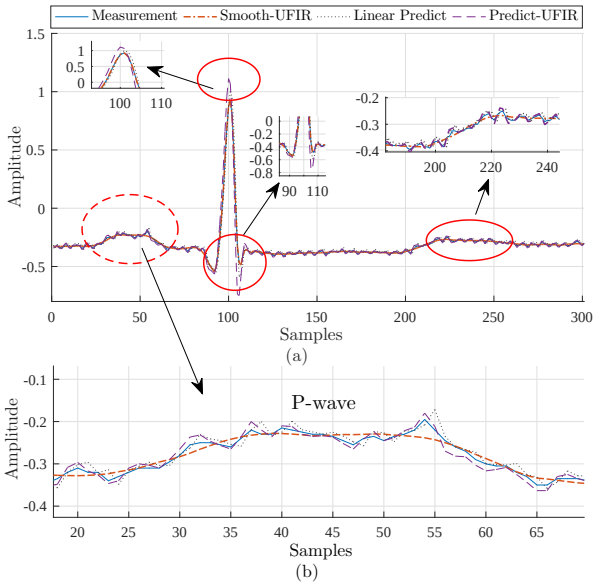

Fig. 3: Errors comparison produced by different estimators: (a) heartbeat estimates: "Smooth-UFIR" is the UFIR smoothing filtering, "Linear Predict" is the linear prediction and "Predict-UFIR" is the UFIR predictive filtering (b) zoomed P-wave of the denoised ECG signal.

estimated as $\hat{\mathrm{R}}$ and a window is introduced with two points, Q' and S'. The estimate $\hat{\mathrm{Q}}$ of Q is obtained by the least value between Q' and $\hat{\mathrm{R}}$. In turn, the estimate $\hat{\mathrm{S}}$ of S is provided by the least value between $\hat{\mathrm{R}}$ and S'. Provided $\hat{\mathrm{Q}}$, $\hat{\mathrm{R}}$ and $\hat{\mathrm{S}}$, the QRS complex is suppressed to save only the P and T waves. Then the estimates $\hat{\mathrm{P}}$ of P and $\hat{\mathrm{T}}$ of T are found similarly by suppressing one of the waves.

Provided $\hat{\mathrm{P}}$, the P wave is split into two segments, P_1 and P_2, where P_1 is extended from the initial point to P_2. In segment P_1, we apply the derivative. Next, we consider a small portion of the resulting signal and find a global maximum. This point is next considered as the beginning of P wave and called $\mathrm{P}_{\mathrm{onset}}$. In segment P_2, we also apply the derivative, consider a small portion of the resulting signal, and find a global minimum. This minimum, which corresponds to the end of P wave, is called $\mathrm{P}_{\mathrm{offset}}$. Values $\mathrm{P}_{\mathrm{onset}}$ and $\mathrm{P}_{\mathrm{offset}}$ are located at points $\mathrm{P}_{\mathrm{p}}^{\mathrm{on}}$ and $\mathrm{P}_{\mathrm{p}}^{\mathrm{off}}$, respectively. Then the duration of P wave is computed as $\mathrm{P}_{\mathrm{dur}} = \mathrm{P}_{\mathrm{p}}^{\mathrm{off}} - \mathrm{P}_{\mathrm{p}}^{\mathrm{on}}$. A distance between $\hat{\mathrm{P}}$ and the baseline is calculated and called the wave amplitude.

4.1 P-Wave Detection Algorithm

A pseudo code of the algorithm designed for the ECG signal features extraction is shown as Algorithm 4.1. Here, ss_i is the smoothed ECG signal; N_{b} is the number of heartbeats; $Baseline$ is a variable, which rep-

resents the reference line; f_s is the data sample frequency; and $Interval$ is a value, which determines the window width to cover Q and S points. The algorithm output consists of estimates of the ECG signal features such as $\hat{\mathrm{P}}$ of P, $\mathrm{P}_{\mathrm{amp}}$ of the P amplitude, $\mathrm{P}_{\mathrm{dur}}$ of the P duration. All these features are extracted from the smoothed signal.

Algorithm 1 A pseudo code of the algorithm to extract morphological features of P-wave

Data: ss_i , N_{b}, $Baseline$, f_s, $Interval$
Result: $\hat{\mathrm{P}}$, $\mathrm{P}_{\mathrm{amp}}$, $\mathrm{P}_{\mathrm{dur}}$.

Begin :
for $i = 1$ to N_{b} **do**
  ss_i= $beatss(i)$
  $\left[\hat{\mathrm{R}}, \mathrm{R}_{\mathrm{p}}\right]$=**max**($ss_i$)
  $[\mathrm{Q}' \quad \mathrm{S}']$ =**IntervalQRS**($ss_i, Interval$)
  $\left[\hat{\mathrm{Q}}, \mathrm{Q}_{\mathrm{p}}\right]$ =**min**($ss_i(\mathrm{Q}' : \mathrm{R}_{\mathrm{p}})$)
  $\left[\hat{\mathrm{S}}, \mathrm{S}_{\mathrm{p}}\right]$=**min**($ss_i(\mathrm{R}_{\mathrm{p}} : \mathrm{S}')$)
  ss_{new}=**suppress**($ss_i(\mathrm{Q}' : \mathrm{S}')$)
  $\left[\hat{\mathrm{P}}, \mathrm{P}_{\mathrm{p}}\right]$=**max**($ss_{new}(1 : \mathrm{Q}')$)
  P_1=$ss_i(1 : \mathrm{P}_{\mathrm{p}})$
  P_2=$ss_i(\mathrm{P}_{\mathrm{p}} : \mathrm{Q}')$
  $\left[\mathrm{P}_{\mathrm{onset}}, \mathrm{P}_{\mathrm{p}}^{\mathrm{on}}\right]$ = **max**(**diff**(P_1))
  $\left[\mathrm{P}_{\mathrm{offset}}, \mathrm{P}_{\mathrm{p}}^{\mathrm{off}}\right]$=**min**(**diff**($\mathrm{P}_2$))
  $Baseline$(1:**length**(ss_i)) = $\mathrm{P}_{\mathrm{offset}}(i)$
  $\mathrm{P}_{\mathrm{amp}}(i)$=$\hat{\mathrm{P}} - Baseline(i)$
  $\mathrm{P}_{\mathrm{dur}}(i)$=$(\mathrm{P}_{\mathrm{p}}^{\mathrm{off}} - \mathrm{P}_{\mathrm{p}}^{\mathrm{on}})/fs$
end for

The algorithm begins with computing $\hat{\mathrm{R}}$ as the ECG signal maximum, using function **max**. Function **IntervalQRS** is applied to compute Q' and S'. The $Interval$ variable determines the window width to cover the QRS complex and obtain $\hat{\mathrm{Q}}$ and $\hat{\mathrm{S}}$ as two minima between Q' and S'. Function **min** is used to find the above-mentioned points. The **supress** function is used to suppress the QRS complex. Function **max** is used to estimate P. Function **diff** is introduced to compute the derivatives in the P_1, P_2 intervals. Functions **max** and **min** with **diff** are used to find $\mathrm{P}_{\mathrm{onset}}$, $\mathrm{P}_{\mathrm{p}}^{\mathrm{on}}$, $\mathrm{P}_{\mathrm{offset}}$, and $\mathrm{P}_{\mathrm{p}}^{\mathrm{off}}$. Provided these values, the duration is estimated of P features. Function **length** is introduced to compute the signal length. The $Baseline$ variable determines the reference line for computing the amplitude features. This variable is equal to $\mathrm{P}_{\mathrm{offset}}$. As can see in the Fig. 4, the estimates provided by the UFIR smoothing filter are more consistent to the average P-wave than by other techniques.

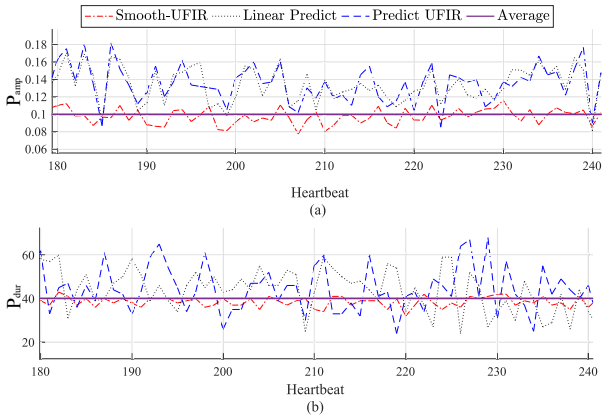

Fig. 4: Applications of different filters to extract the ECG amplitude features: (a) amplitud of P-wave and (b) duration of P-wave. Here "Smooth-UFIR" is the UFIR smoothing filter, "Predict UFIR" is the linear predictor and "Predict -UFIR" is the UFIR predictive filter.

5 Validation of P-Wave Feature Estimates

Because the positive-valued P-values vary for normal and abnormal heartbeats in a wide range, it is required to specify the confidence interval for the P-wave estimate to be valid with a given probability. We do it by using the Rice probability density function (pdf), which corresponds to the envelop of a harmonic signal in Gaussian noise [27, 28],

$$p(r) = \frac{r}{\sigma^2}\exp\left(-\frac{r^2+A}{2\sigma^2}\right) I_0\left(\frac{Ar}{\sigma^2}\right), \qquad (24)$$

where σ^2 is the variance of acting noise, A is the harmonic signal amplitude, and $I_0(x)$ is the modified Bessel function of the first kind and zeroth order. The normalized Rice pdf is given by

$$p(v) = v\,\exp\left(-\frac{v^2+a^2}{2}\right) I_0(Av), \qquad (25)$$

where $v = \frac{r}{\sigma}$ and $a = \frac{A}{\sigma}$. Note that (25) reduces to the Rayleigh distribution [29] when $a = 0$ and, by large a, it becomes Gaussian.

5.1 Confidence Interval for P-Wave

To specify the confidence interval for the P-wave estimates provided by Algorithm 4.1, we have investigated the P-wave histograms for normal and abnormal heartbeats taken from different persons as shown in Fig. 5. We employed a register of different ages between female and male gender with

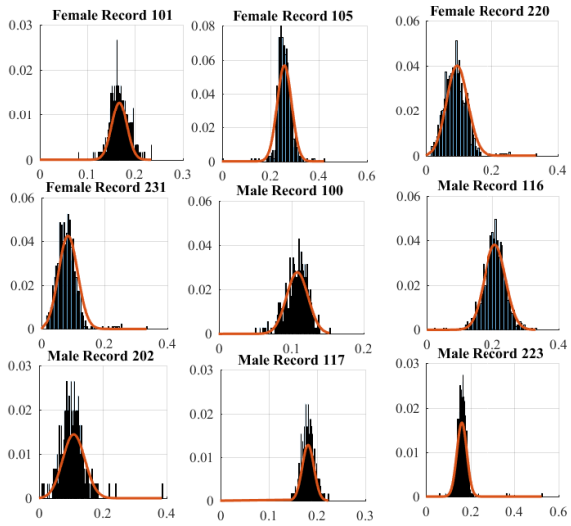

Fig. 5: Normalized histograms and Rice-based approximations for P-wave features of healthy heartbeats.

9159 healthy and 2540 APC beats. The name of the signal is referenced based on the Arrhythmia database. In this case the records used are $[101,\ 105,\ 220,\ 231,\ 100,\ 116,\ 202,\ 117,\ 223]$. Other registers were also processed, but we select only those records, which are most close to the reference signal. The number of bins varies for each histogram between 500 and 1000. Also, we consider more representative features, because the ECG record has a considerable variability. Values v and a for the Rice pdf were chosen in the minimum MSE sense.

5.1.1 Confidence Interval for Normal Heartbeats

As can seen in the Fig. 6, the confidence interval (CI) for the APC heartbeats has two boundaries, 0.009 and 0.125, with the probability of 76.33%. For healthy beats, the boundaries were found to be 0.1403 and 0.3074.

6 Conclusions

In this paper, we have presented the UFIR smoothing filter as an estimator of the ECG signal features and shown that it has better performance than the known predictive and filtering solutions. We also specified the confidence interval for the ECG heartbeats using the Rice-based approximation of the P-wave distribution. Because the confidence intervals specified for expert's probabilities play a key role in automatic diagnosis of heart diseases, we consider this topic as a next important part of our work.

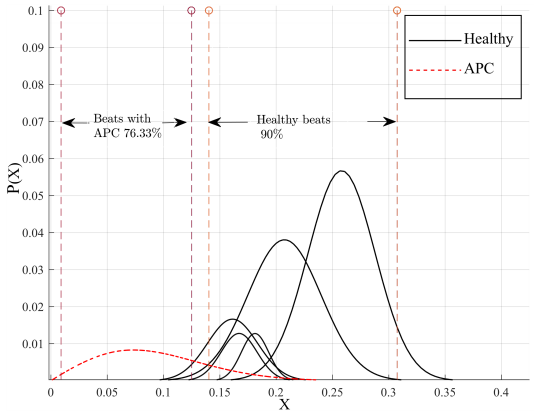

Fig. 6: Confidence intervals for APC (sold) and healthy (dashed) ECG heartbeats.

References:

[1] R. Joy, U.R. Acharya, K.M Mandana, A.K. Ray and C. Chakraborty, Expert systems with applications of principal component analysis to ECG signals for automated diagnosis of cardiac health, *Expert Systems With Applications*, Vol. 39, 2012, pp. 11792–11800.

[2] R.B. Rao PB, Singh N, Ann Card Anaesth, Dexmedetomidine induced atrial premature complex' *Ann Card Anaesth*, Vol.19, 2016, pp. 347–350.

[3] L. Biel, O. Pettersson, L. Philipson, and P. Wide, ECG analysis: a new approach in human identification, *IEEE Trans. Instrum. Measur.*, Vol. 50, 2001, pp.808–812.

[4] S.C. Fang and H.L Chan,Human identification by quantifying similarity and dissimilarity in electrocardiogram phase space, *Pattern Recognition*, Vol. 42, 2009, pp.1824–1831.

[5] A.D.C. Chan, M.M. Hamdy, A. Badre and V Badee, 'Wavelet distance measure for person identification using electrocardiograms, *IEEE Trans Instrum Measur*,Vol. 57, 2008, pp. 248–253.

[6] J. Wang, and M. She, and S. Nahavandi and A. Kouzani, Human identification from ECG signals via sparse representation of local segments, *IEEE Signal Process. Lett.*, Vol. 20, 2013, pp. 937–940.

[7] F. Gargiulo, A. Fratini, M. Sansone, Mario and C. Sansone, Subject identification via ECG fiducial-based systems: Influence of the type of QT interval correction, *Comput. Methods and Programs in Biomedicine*, Vol. 212 ,2015, pp.127–136.

[8] U.R. Acharya, H. Fujita, V.K. Sudarshan, S. Lih, M. Adam, *et. al.*, Knowledge-based systems automated detection and localization of myocardial infarction using electrocardiogram: a comparative study of different leads',*Knowledge-Based Systems*, Vol. 99, 2016, pp.146–156.

[9] R.J. Martis, U.R. Acharya, and H. Adeli, Current methods in electrocardiogram characterization,*Computers in Biology and Medicine*, Vol. 48, 2014, pp.133–149.

[10] B.N. Singh, and A.K. Tiwari, Optimal selection of wavelet basis function applied to ECG signal denoising, *Digital Signal Processing*, Vol. 16, 2006, pp. 275–287.

[11] Y. S. Shmaliy, An unbiased FIR filter for TIE model of a local clock in applications to GPS-based timekeeping, *IEEE Trans. Ultrason., Ferroelect., and Freq. Control*, No. 5, Vol. 53, 2006 pp. 862–869.

[12] A. Savitzky, and M. J. E. Golay, Smoothing and differentiation of data by simplified least squares procedures, *Analytical Chemistry*, No. 8, Vol. 36,1964, pp.1627–1639.

[13] Y. S. Shmaliy and O. Ibarra-Manzano, Optimal and unbiased FIR filtering in discrete time state space with smoothing and predictive properties, *EURASIP Journal on Advances in Signal Processing*, Vol.1, 2012.

[14] Y. S. Shmaliy and L. J. Morales-Mendoza, "FIR smoothing of discrete-time polynomial signals in state space", *IEEE Trans. Signal Process.*, No. 5, Vol. 58,2010, pp. 2544-2555.

[15] Y. S. Shmaliy and O. Ibarra-Manzano, and Arceo-Miquel, Luis and J. Munoz-Diaz, A thinning algorithm for GPS-based unbiased FIR estimation of a clock TIE model, *Measurement*, No. 5, Vol. 41, 2008 pp 538–550.

[16] S. Hargittai, Savitzky-Golay least-squares polynomial filters in ECG signal processing, *Computers in Cardiology*, Vol. 32,2005, pp. 763–766.

[17] S.R. Krishnan, and C.S Seelamantula, On the selection of optimum Savitzky-Golay filters, *IEEE Trans. Signal Process.*, No. 2, Vol. 61, 2013, pp.380-391.

[18] G. B. Moody and R. G. Mark, The impact of the MIT-BIH arrhythmia database, *IEEE Eng. Med. Biol. Mag.*, No 3, vol. 20, 2001, pp. 45–50.

[19] A.L. Goldberger, L.A.N Amaral, L. Glass, J. M. Hausdorff, P.C. Ivanov, R.G. Mark, J.E. Mietus, G.B Moody, C.K. Penk and H. E. Stanley, PhysioBank, PhysioToolkit, and PhysioNet components of a new research resource for complex physiologic signals, *Circulation*, Vol.101, 2000, pp. 215–220.

[20] Y. S. Shmaliy, An unbiased p-step predictive FIR filter for a class of noise free discrete-time models with independently observed statess,*Signal, Image and Video Processing*, No. 2, Vol. 3, 2009, pp. 127–135.

[21] L. Morales-Mendoza, and H. Gamboa-Rosales and Y. S. Shmaliy fitting of finite data, A new class of discrete orthogonal polynomials for blind, *Signal Processing*, No. 7, Vol. 93, 2013, pp. 1785-1793.

[22] H. Gamboa-Rosales, and L. Morales-Mendoza and Shmaliy, Y. S. Shmaliy, Unbiased impulse responses: A class of discrete orthogonal polynomials,*ICIC Express Letters*, Vol. 7, 2013, pp. 2005-2010.

[23] C. Lastre-Dominguez , Y.S. Shmaliy and O. Ibarra-Manzano, and L.J. Morales-Mendoza, Unbiased FIR denoising of ECG signals, *2017 14th International Conference on Electrical Engineering, Computing Science and Automatic Control (CCE)*(2017)pp. 1–6.

[24] John Makhoul, Linear prediction: A review, *IEEE*, 1975, pp. 561-580.

[25] K. P Lin, and W.H. Chang, QRS feature extraction using linear prediction., *IEEE Trans. Biomed. Eng.* Vol. 36, 1986, pp. 1050–1055.

[26] J. Pan, Jiapu and W.J. Tompkins, Willis, A real-time QRS detection algorithm, *IEEE Trans Biomed. Eng.*, Vol. 32,1985, pp. 230–236.

[27] S. Haykin, Communication Systems, *Wiley*, (2001).

[28] Y.S. Shmaliy, Limiting phase errors of passive wireless SAW sensing with differential measurement, *IEEE Sensors Journal*, Vol.4, 2004, pp.819-827.

[29] G. Stock, Rician Envelope Estimation and Confidence Intervals in Low Signal/Noise Levels, *IEEE Electronics Letters*, Vol.23,1987,pp, 832–834.